Catalysis Today 176 (2011) 373–382

Contents lists available at ScienceDirect

Catalysis Today

journal homepage: www.elsevier.com/locate/cattod

Applicability of membrane reactor for WGS coal derived gas processing: Simulation-based analysis

Krzysztof Gosiewski*, Marek Tańczyk

Institute of Chemical Engineering, Polish Academy of Sciences, ul. Bałtycka 5, 44-100 Gliwice, Poland

ARTICLE INFO

Article history:
Received 27 August 2010
Received in revised form
15 November 2010
Accepted 16 November 2010
Available online 18 December 2010

Keywords:
Membrane reactors
WGS reaction
Mathematical model
Simulation
Coal gasification
Hydrogen separation

ABSTRACT

Gas from coal gasification contains less hydrogen than from other syngas production methods. An attractive option is its further hydrogen enrichment for pure hydrogen production in a membrane reactor (MR) by water gas shift (WGS). The goal of the present study was to analyse MR fed with coal derived gas. Simulations for feasible membrane permeation parameters revealed that to get high conversion above 90% a relatively high S/C should be applied. Moreover, hydrogen recovery is in this case low (below 30%) so for hydrogen production an additional H_2 separation after the MR should have been applied. The paper also shows that a clear advantage of counter- over co-current flow configuration in MR appears only for low pressure in the reaction zone. The realistic feasible Pd–Cu–Ni membrane parameters result in a rather large membrane area, thus possible heat exchange between the reaction and permeation zone can have important influences on temperature profiles in the MR. This cooling effect could lessen excessive temperature increase in the reaction zone. Results for other than single step MR configurations are also presented in the paper. It is stated in conclusion that future successful application of MRs for coal-derived gas depends on development of not only new catalysts with adequately wide operational temperature range, but also membranes with a high enough permeability.

1. Introduction

Extensive studies on the coal gasification as an element of clean coal technologies are carried out recently, especially in coal dependent countries. The goal of the present study is to find answer to a question: is it worth to use a membrane reactor (MR) for processing of the gas from coal gasification and, moreover, are suitable membranes and/or industrial catalysts available at present to be applied soon in the industrial practice? As the study is preliminary in nature, mathematical simulations seemed to be a proper approach. First attempt was already published in [1] but the study reported in [1] was carried out assuming unrealistically high membrane permeation. Thus the study was extended in the present paper by examining the case when a feasible (realistic) membrane permeation is assumed in the simulation. The results presented in this paper are, however, less optimistic than those, in the previous study [1]. Numerous studies appeared recently on membrane reactors (MRs) for WGS reaction accompanied by the simultaneous separation of one of its products, H_2 or CO_2, alternatively. The relevant literature concerning membrane reactor (MR) models is abundant; thus we shall mention here some chosen examples only. The models are mostly steady-state, one-dimensional in space e.g. [2–9], but two-dimensional including axial and radial gradients are also used [10,11]. Dynamic models can also be found, but for reactors operating in the permanent unsteady state e.g. for the reverse-flow MR syngas production [12–14]. Majority of papers describe tube and shell reactor configuration with reaction zone either in the tube or in the shell, but a case of fluidized MR for ultrapure hydrogen production is also analysed in [15,16]. Some models assume isothermal MR operation [2,4,5,8] while the other include heat or enthalpy balances, allowing to simulate non-isothermal or adiabatic operation, what is much more suitable for exothermal WGS reaction. Studies [2,4–7,11] directly concern WGS reaction. Simulations presented in [4–6] were carried out for kinetic data of Cu–Zn low temperature catalyst, while in [7,11] for high temperature Fe–Cr catalyst. Kinetic data based on own investigation of the authors or were taken from the literature. A very simple model presented in [2] assumes that WGS reaction kinetics is faster than the hydrogen permeation flux rates (porous membrane is assumed) allowing the feed (retentate) side to be in dynamic equilibrium, therefore in consequence problem of kinetic may be entirely omitted. Simulation results presented in the cited studies concerning WGS reaction mostly assume Pd or Pd alloys composite membranes. Authors from

Abbreviations: CG, coal gasification derived gas composition given in Table 3; GHSV, gas hourly space velocity (h^{-1}); HTC, high temperature catalyst; LTC, low temperature catalyst; MR, membrane reactor; TZC-3/1, commercial polish high temperature catalyst symbol; TMC-3/1, commercial polish low temperature catalyst symbol.

* Corresponding author. Tel.: +48 601 546535; fax: +48 324 010124.
E-mail address: k.gosiewski@iich.gliwice.pl (K. Gosiewski).

0920-5861/$ – see front matter © 2010 Elsevier B.V. All rights reserved.
doi:10.1016/j.cattod.2010.11.042

Nomenclature

C_{pt}, C_{ps}	specific heat of fluid in tube and shell, respectively ($J\,mol^{-1}\,K^{-1}$)
DFE	distance from equilibrium given by formula (2).
DFE_{in}, DFE_{out}	distance from equilibrium at the inlet and outlet of the reaction zone (tube)
E_{cat}	activation energy for catalyst in Eq. (12) ($J\,mol^{-1}$)
E_{perm}	permeation activation energy ($J\,mol^{-1}$)
F_{ti}, F_{si}	molar flow rate of component *i* in tube and in shell, respectively ($mol\,s^{-1}$)
F^{out}_{t,H_2}, F^{out}_{s,H_2}	molar flow rate of hydrogen on the outlet from tube or shell, respectively ($mol\,s^{-1}$)
h_{t-s}, h_{surr}	tube to shell and shell to surroundings heat transfer coefficients, respectively ($W\,m^{-2}\,K^{-1}$)
ΔH	heat of reaction ($J\,mol^{-1}$)
J_{H_2}	molar flux of hydrogen through membrane ($mol\,s^{-1}\,m^{-2}$)
$k(T)$	reaction rate constant ($mol\,s^{-1}\,kg^{-1}\,Pa^{-0.65}$)
k_0	pre-exponential factor in Eq. (12) ($mol\,s^{-1}\,kg^{-1}\,Pa^{-0.65}$)
K_p	equilibrium constant
L	reactor length (m)
L_1, L_2, L_3	reactor section nos. 1, 2, 3, respectively (m)
m	exponent in Eqs. (8) and (9): $m=1$ for counter-current; $m=2$ for co-current reactor
n	exponent in Eq. (4)
p_{mH_2}	permeability coefficient of hydrogen ($mol\,m^{-1}\,s^{-1}\,Pa^{-n}$)
$p_{mH_2,0}$	pre-exponential factor in Eq. (5) ($mol\,m^{-1}\,s^{-1}\,Pa^{-n}$)
P_{ti}, P_{si}	partial pressure of component "*i*" in tube and in shell, respectively (Pa)
P	total pressure in the reaction zone (Pa)
Q_p	term given by Eq. (11)
R	gas constant ($J\,mol^{-1}\,K^{-1}$)
R_1, R_2, R_3	inner and outer radius of tube and inner radius of shell, respectively (m)
r_{CO}	rate of reaction given by Eq. (10) ($mol\,s^{-1}\,kg^{-1}$)
$r_{CO_{max}}$	maximum value of the reaction rate (10) in the reaction zone (tube) ($mol\,s^{-1}\,kg^{-1}$)
R_{H_2}	hydrogen recovery factor given by formula (3).
S/C	steam to carbon ratio
T_t, T_s, T_{surr}	tube, shell and surroundings temperature (K or °C)
T	temperature (K)
T_{in}, T_{out}	temperature at the inlet and outlet of the reaction zone (tube) (K or °C)
ΔT	total temperature increase in the reaction zone (tube) (K)
$V_{G_{in}}$	inlet feed gas flowrate to the reactor (dm^3 (STP) s^{-1})
$V_{S_{in}}$	inlet steam flowrate to the reactor (dm^3 (STP) s^{-1})
V_{sweep}	inlet sweep gas flowrate (dm^3 (STP) s^{-1})
X	carbon monoxide final conversion
z	axial coordinate (m)
δ	membrane thickness (m)
ρ_B	bulk density of catalyst in tube ($kg\,m^{-3}$)

US Department of Energy (US DOE) [2] analysed for WGS reactor inorganic porous membrane, but due to poor hydrogen selectivity such a solution occurred to be not especially advantageous. Thus in more recent study e.g. [17] US DOE decided to develop an inorganic composite palladium-based MR module. In model simulations authors used to apply very different pressures in the reaction zone from 0.1 to 3 MPa (1–30 bar), while conventional industrial WGS reactors operates with pressures as high as 7 MPa (70 bar). Obviously, due to membrane resistance pressure in the retentate side may not be too high, but pressures above 2 MPa should necessarily be considered for MR in this case, however. Recently WGS MR technology is considered as an element of IGCC power plant [18,19] so the coal-derived gas processing in MRs is a very actual subject.

The WGS MR processing such gas can be applied generally for the two different industrial goals:

- hydrogen enrichment of the coal gasification gas to adjust the syngas H_2/CO ratio for demands of an appropriate chemical synthesis (e.g. to Fisher Tropsch, methanol synthesis, etc.);
- pure hydrogen production.

It seems that the second case should be more economically attractive for coal-derived gas processing, so that the aim of the present study was to find, how far MRs are suitable in this application. As it was already presented in [1] composition of the feed gas for WGS reactor derived from hydrocarbons (mainly methane) processing is clearly different from that derived from coal gasification, generally when the ratio H_2/CO is taken into account. For coal-derived gas the H_2/CO ratio at the inlet to WGS comprises in the range of 0.5–1.15 and is significantly lower than that for the other technologies, up to 5 for methane steam reforming. Therefore, due to lower amount of the WGS reaction product (H_2) in the feed, the reaction is less equilibrium limited, when comparing with the conventional sources of syngas.

On the other hand, higher CO content, exceeding even 60% in some gasification technologies, may lead to much higher overall catalyst temperature increase in the MR. Thus, study presented in [1] revealed that none of existing commercial catalysts is directly appropriate for the one-stage membrane WGS reactor due to their too narrow temperature range of operation. Mathematical model of such a membrane reactor and results of simulation studies presented in [1] were promising for future applications, but the simulations were carried out, however, assuming very high hydrogen permeability through the membrane. The present study is a continuation of the previous simulations presented in [1], but for more realistic, feasible membrane parameters.

2. A brief description of the mathematical model

The model was developed for the "tube in tube" configuration, though extension of simulation results for shell and multi-tube type is not difficult, however. Simplified sketch of the MR is shown in Fig. 1a. The reaction zone is packed with the catalyst inside the inner tube; this tube is made of membrane material separating product of WGS reaction to the outer tube (shell). To the shell side an inert sweep gas can be introduced either in co-current or in counter-current configuration with respect to the flow direction in the tube. Membranes for the discussed case of WGS reactor should be proof against high temperature and high pressure in the reaction zone. Thus in [1] and also in the present study only H_2 selective membranes, containing Pd or its alloys were taken into account. A brief description of the model was already given in [1], so it will not be repeated here in details. A graphic outline of phenomena included in the model is shown in Fig. 1b. General form of the model equations is given in Table 1.

Generally the model is similar to the 1D model published by Kumar et al. [9]. However, the comprehensive model presented there was reduced in the present study by assumption

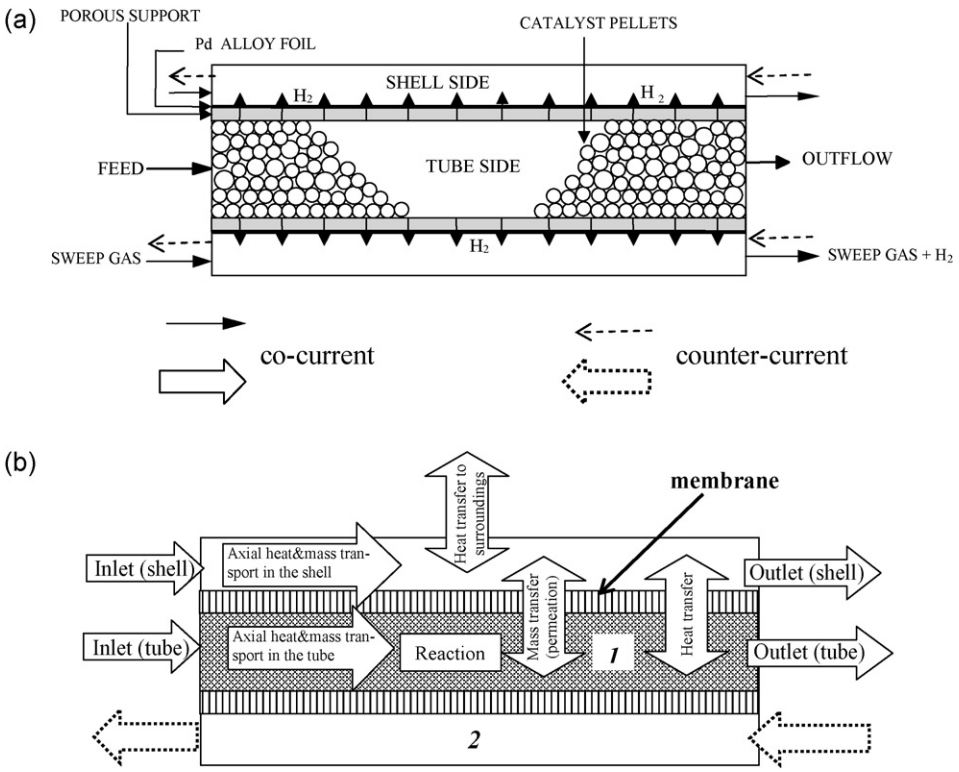

Fig. 1. Graphic outline of the MR (a) and phenomena included in the mathematical model of the MR (b). 1 – Tube side (reaction zone), 2 – shell side (permeation zone).

that the reaction occurs on the tube side only. The momentum balance equations were also neglected, since constant values of pressure along the tube and shell length were assumed for preliminary studies. The model was extended, however, by adding separate heat balances for the tube and shell side, thus avoiding some simplifying assumption made by Kumar et al. [9] (equal temperatures in the tube and shell, i.e. neglecting the heat exchange between them and assuming negligible heat loss to surroundings).

Since CO does not permeate through the Pd membrane, the final CO conversion in MR can be defined as:

$$X = \frac{F^{\text{in}}_{\text{t,CO}} - F^{\text{out}}_{\text{t,CO}}}{F^{\text{in}}_{\text{t,CO}}} \tag{1}$$

Because the WGS reaction is equilibrium controlled a distance from equilibrium DFE was defined as:

$$\text{DFE} = 1 - \frac{P_{\text{t,H}_2} \times P_{\text{t,CO}_2}}{K_{\text{p}} \times P_{\text{t,CO}} \times P_{\text{t,H}_2\text{O}}} \tag{2}$$

DFE ≈ 1 when the reaction rate is not decreased by equilibrium, while tends to zero when the reaction extinguishes (reaches an equilibrium state).

Obviously the final CO conversion X (Eq. (1)), the DFE (Eq. (2)) and the hydrogen recovery factor given by the formula:

$$R_{\text{H}_2} = \frac{F^{\text{out}}_{\text{s,H}_2}}{F^{\text{out}}_{\text{t,H}_2} + F^{\text{out}}_{\text{s,H}_2}} \tag{3}$$

were carefully analysed for all simulated variants.

Table 1
Basic formulae of the mathematical model.

	Molar balances for reactive component i	Heat balances
Tube	$\frac{dF_{ti}}{dz} \pm \pi R_1^2 \rho_B (r_{CO}) + 2\pi R_1 J_i = 0$ (6)	$F_t C_{pt} \frac{dT_t}{dz} = -\left[\pi R_1^2 \rho_B \Delta H r_{CO} + \pi \frac{R_1 + R_2}{2} h_{t-s}(T_t - T_s)\right]$ (7)
	Boundary conditions: $F_{ti} = F_{ti0}$ for $z = 0$	$T_t = T_{t0}$ for $z = 0$
Shell	Balance only for hydrogen: $(-1)^m \frac{dF_{s,H_2}}{dz} - 2\pi R_2 J_{H_2} = 0$ (8)	$(-1)^m F_s C_{ps} \frac{dT_s}{dz} = \pi \frac{R_1 + R_2}{2} h_{t-s}(T_t - T_s) - \pi R_3 h_{surr}(T_s - T_{surr})$ (9)
	Boundary conditions: $F_{s,H_2} = 0$ for $z = 0$ (co-current); $F_{s,H_2} = 0$ for $z = L$ (counter-current)	$T_s = T_{s,0}$ for $z = 0$ (co-current) $T_s = T_{s,0}$ for $z = L$ (counter-current)
Kinetics	Kinetic equation for TZC-3/1 high temperature catalyst used in the present simulations	
	$r_{CO} = k(T) \times \frac{P_{t,CO} P^{0.1}_{t,H_2O}}{P^{0.3}_{t,CO_2} P^{0.15}_{t,H_2}} \times \left(1 - \frac{Q_p}{K_p}\right)$ (10)	where $Q_p = \frac{P_{t,H_2} \times P_{t,CO_2}}{P_{t,CO} \times P_{t,H_2O}}$ (11) and $k(T) = k_0 \exp\left(\frac{-E_{cat}}{R \times T_t}\right)$ (12)

A simulation tool PSE gPROMS ModelBuilder 3.1.3 [20] was used for the implementation of the model. A computer program was developed using an equation oriented gPROMS language. The model took advantage of physical properties data bases and numerical procedures (discretization schemes) for differential equations built into the gPROMS package. The gPROMS offers a bunch of options of discretization methods. In the present study the most often the Centered Finite Difference Method (CFDM) was used, but sometimes in the cases of appearing numerical instabilities some other methods were tried.

Physical properties (e.g. heat capacities of gaseous streams) of media in MR were calculated using the "Ideal Physical Properties Foreign Object (IPPFO)" [21] built into the gPROMS package, while the heat of reaction and the reaction equilibrium constant were calculated using the formulas for standard enthalpies and entropies used in the Chemkin system [22].

3. MR simulation for coal derived gas feed and feasible membrane permeation parameters

3.1. Simulations overview

Simulations for membrane with very high H_2 permeability published in [1] were optimistic. E.g. for moderate S/C = 2.43 high CO conversion and high hydrogen recovery (both well above 90%) could have been obtained. Being aware that it could have been a result of the overestimated membrane permeability, some more realistic membrane parameters were selected for further study. Since membrane in the WGS MR should operate in high temperature and pressure a search for the feasible membrane parameters to be used in simulations has to take into account operating temperature and trans-membrane pressure difference in which a membrane was investigated. Bibliographic scrutiny allowed to select the membrane parameters published in [23] which were used in the present simulations as a feasible H_2 permeation case, because similarly as in [1], only H_2 separation option by using Pd and Pd alloy composite membranes was taken into account. It was assumed that the following Sievert's type formula describes permeation for these membranes:

$$J_{H_2} = \frac{p_{mH_2}}{\delta}[P^n_{t,H_2} - P^n_{s,H_2}] \quad (4)$$

where a permeation coefficient is given by the Arrhenius type formula as a function of temperature:

$$p_{mH_2} = p_{mH_2,0} \quad \exp\left(\frac{-E_{perm}}{RT}\right) \quad (5)$$

Membrane parameters used in the present simulation are listed in Table 2.

Pre-exponential factor $p_{mH_2,0}$ given in Table 2 was recalculated to notation used in the present study from the source data given in [23]. Membrane deposited on the porous nickel support, as further simulations revealed, can have additional advantage for the case discussed. Metallic support could possibly enhance heat conduction through membrane that is advantageous for the temperature profile along the MR because it can reduce maximum temperature in the reaction zone.

Basic MR parameters and kinetic data for the catalysts used in simulations were substantially the same as in [1], where simulations were carried out for industrial low temperature catalyst (LTC) Cu–Zn with commercial symbol TMC-3/1 and high temperature catalyst (HTC) Fe–Cr–Cu with symbol TZC-3/1 (cf. [24]). Kinetic equation for this catalyst (cf. [25]) is also given in Table 1. Values of the parameters necessary to calculate reaction rate r_{CO} were obtained for the present study by courtesy of the industrial catalyst producer [24], but unfortunately without a permission for publishing these data due to commercial reasons. In the present study simulations were performed for HTC and LTC as well, but due to discussed in [1] low reliability of kinetic data for LTC only results for HTC are presented in this paper.

The only important difference in the present results is that the simulations were carried out for more realistic membrane permeation parameters given in Table 2. The other basic parameters used in the simulations are listed in Table 3.

Summary of the most interesting present simulation results is given in Table 4. It occurred, that for the membrane parameters in this case, lower flow rates in the reaction zone should have been applied in order to get high enough conversion ratio (above 90%). Thus GHSV occurred to be lower than values presented in [1] where for HTC reached over 47,000 h^{-1}, while at the present study the highest value obtained in simulations was approx. 12,400 h^{-1} (detailed data are given in Table 4), but still higher than in conventional reactor fed with CG composition. On the other hand, in order to get conversions higher than 90% S/C ratio must be somewhat higher. Because the WGS reaction is equilibrium controlled, both the input and output values of DFE are given in Table 4. Moreover, since the current reaction rate r_{CO} along the MR length is strongly influenced by the current

Table 2
Parameters of feasible membrane used in the present simulation (selected according to literature [23]).

Quantity	Value
Membrane material	Pd–Cu–Ni on porous nickel support
Exponent n in Eq. (4)	0.6
Membrane thickness δ	4 μm
Pre-exponential factor in Eq. (5) $p_{mH_2,0}$	1.85×10^{-9} mol m^{-1} s^{-1} Pa^{-n}
Activation energy in Eq. (5) E_{perm}	13,500 J mol^{-1}
Maximum membrane temperature	500 °C

Table 3
Basic parameter values used in the simulations.

Quantity	Value
Inner radius of tube R_1	2.0 cm
Outer radius of tube R_2	2.2 cm
Inner radius of shell R_3	2.8 cm
Total pressure in reaction side (tube)	2.6 MPa (26 bar)
Total pressure in permeate side (shell)	0.1013 MPa (~1 bar)
Temperature of the surroundings T_{surr}	20 °C
Sweep gas flow rate V_{sweep}	1 dm^3 (STP) s^{-1}
Sweep gas inlet temperature	20 °C
Feed coal gasification (CG) gas i.e. composition as for SHELL or PRENFLO technology[a]	Vol% on dry basis
CO	61.6
CO_2	1.7
H_2	30.6
N_2 + Ar	4.8
Others	1.3
WGS catalyst description for which kinetic data were supplied by the catalyst producer	
HTC (TZC-3/1) producer's basic data	
Fe_2O_3	Min 71.5 wt%
Cr_2O_3	Min 7.3 wt%
CuO	Min 1.25 wt%
Graphite	~2 wt%
Shape: tablets (diameter × height)	6 mm × 6 mm
Bulk density of catalyst ρ_B	1250 kg m^{-3}

Heat capacities of gaseous streams in the tube and shell were calculated using the "Ideal Physical Properties Foreign Object (IPPFO)" built into the gPROMS package. Heat of reaction and the reaction equilibrium constant were calculated using the formulas for standard enthalpies and entropies used in the Chemkin system [22].

[a] Inlet CG gas and steam flowrates for every item are given in Table 4.

Table 4
Summary of the MR simulations performed for the feasible membrane with the high temperature catalyst (HTC).

No.		Option	L [m]	$V_{S_{in}}$ [dm^3/s]	$V_{G_{in}}$ [dm^3/s]	GHSV [1/h]	S/C [–]	X [–]	T_{in} [°C]	T_{out} [°C]	ΔT [K]	DFE_{in} [–]	DFE_{out} [–]	r_{COma} [mol/(kg s)]	R_{H_2} [–]
1	Counter-current	MR with heat transfer coefficients h_{t-s}, $h_{surr} = 10\,W\,m^{-2}\,K^{-1}$ and higher steam flow rate	3.3	5.0	1.5	12,414	5.41	0.9509	310	406	96	0.9999	0.5834	0.0124	0.275
2		MR with heat transfer coefficients h_{t-s}, $h_{surr} = 10\,W\,m^{-2}\,K^{-1}$ and lower steam flow rate	2.2	4.0	2.0	7813	3.25	0.9214	310	471	161		0.0763	0.0317	0.206
3		MR with heat transfer coefficients h_{t-s}, $h_{surr} = 5\,W\,m^{-2}\,K^{-1}$ and higher steam flow rate	3.4	5.0	1.5	5477	5.41	0.9682	310	428	118		0.1916	0.0146	0.284
4		MR as above, but with pressure 0.21 MPa in the reaction zone	12.0	5.0	1.5	1552	5.41	0.8233	325	370	45		0.9287	0.0028	0.137
5		MR with heat transfer coefficients h_{t-s}, $h_{surr} = 5\,W\,m^{-2}\,K^{-1}$ with lower steam flow rate	2.2	4.0	2.0	7813	3.25	0.9154	310	487	177		0.0361	0.0353	0.201
6		MR without radial heat transfer and with lower steam flow rate	2.2	4.0	2.0	7813	3.25	0.9037	310	507	197		0.0134	0.0398	0.180
7	Co-current	MR with heat transfer coefficients h_{t-s}, $h_{surr} = 10\,W\,m^{-2}\,K^{-1}$ and lower steam flow rate	2.2	4.0	2.0	7813	3.25	0.9175	310	470	160	0.9999	0.1235	0.0276	0.199
8		MR with heat transfer coefficients h_{t-s}, $h_{surr} = 5\,W\,m^{-2}\,K^{-1}$ and higher steam flow rate	3.4	5.0	1.5	5477	5.41	0.9488	305	422	117		0.5298	0.0118	0.263
9		MR as above, but with pressure 0.21 MPa in the reaction zone	12.0	5.0	1.5	1552	5.41	0.6288	325	345	20		0.9843	0.0028	0.151

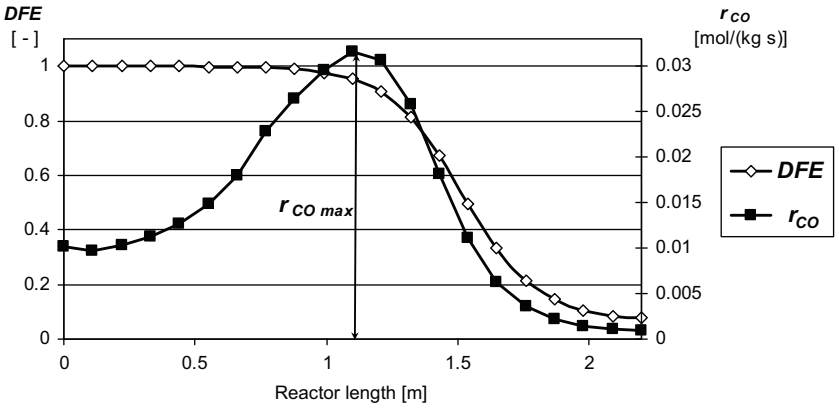

Fig. 2. Distance from equilibrium DFE given by Eq. (2) and reaction rate r_{CO} given by Eq. (10) profiles along the reaction zone as an example (cf. item 2 in Table 4) of strongly equilibrium controlled MR process.

DFE value, a maximum value $r_{CO_{max}}$ of the reaction rate is also included.

Fig. 2 illustrates both DFE and r_{CO} profiles along the reactor as an example. The results reveal that due to lower, but realistic permeation stream, in spite of lower GHSV, MR should be longer (thus the membrane surface larger) in order to obtain the required conversion. For practically acceptable S/C = 3.25 (cf. items 2, 5, 6, and 7 in Table 4) low values of DFE_{out} mean that at the MR outlet WGS reaction is very close to equilibrium. The main drawback, however, consists in relatively low hydrogen recovery R_{H_2} (within the range 15–20%). Even when applying higher S/C = 5.41 (cf. items 1, 3, and 8 in Table 4) R_{H_2} hardly exceeds 28%, while for the very high membrane permeability assumed in [1] achievement of hydrogen recovery well above 90% seemed to be very easy.

Every simulation in this part of the study was carried out assuming sweep gas flow rate $V_{sweep} = 1\ dm^3\ (STP)\ s^{-1}$.

3.2. Heat exchange effect in MR

It occurred that due to large membrane surface, cooling effect by the heat exchange from tube to shell and from shell to surroundings becomes to be significant when the excessive temperature increase in the reaction zone is taken into account. The heat exchange entails that the temperature profile may not be necessarily monotonic, since a maximum value might appear before the end of the bed, as shown in Fig. 3. Thus problems lessen when comparing with the results in [1] for high membrane permeance. They could appear again when H_2 permeability will be higher in the future. Thus, there is a clear contradiction between the catalyst operational temperature range and separation properties of the membrane. For low H_2 permeability cooling of MR by the sweep gas flow could be an element of future process optimization. Calculation of the heat transfer coefficient in MRs, especially the value through the membrane h_{t-s} is a difficult task and demands knowledge hardly available, about the heat transfer parameters of the membrane and its support. A rough estimation allows us to predict that obviously this coefficient is not very high. A widely cited paper [26] estimates this coefficient to be as low as $2.4\ W\ m^{-2}\ K^{-1}$ but one can expect that if a metallic support would be considered this coefficient could be a little higher, but one cannot expect that higher than $10\ W\ m^{-2}\ K^{-1}$. The coefficient to surroundings h_{surr} is also small due to the low sweep gas flow velocity and, moreover, it has negligible influence since the temperature difference between the fluid in the shell and surroundings is small too. To estimate roughly the influence of the radial heat exchange in MR it was assumed that the both coefficients are equal and can have values in the range between 0 and $10\ W\ m^{-2}\ K^{-1}$. Namely the simulations were carried out optionally for $h_{t-s} = h_{surr} = 0$, 5 and $10\ W\ m^{-2}\ K^{-1}$. Simulations allow for comparison of results calculated for these different heat transfer coefficients but the same remaining data introduced for simulations. From Table 4 is clearly visible that the higher heat transfer coefficients (h_{t-s} and h_{surr}) the lower temperature increase (ΔT) in MR (compare items 2 with 5 and 6 or 1 with 3 in Table 4). Unfortunately neither conversion ratio X nor hydrogen recovery R_{H_2} increase significantly with increased heat transfer through membrane.

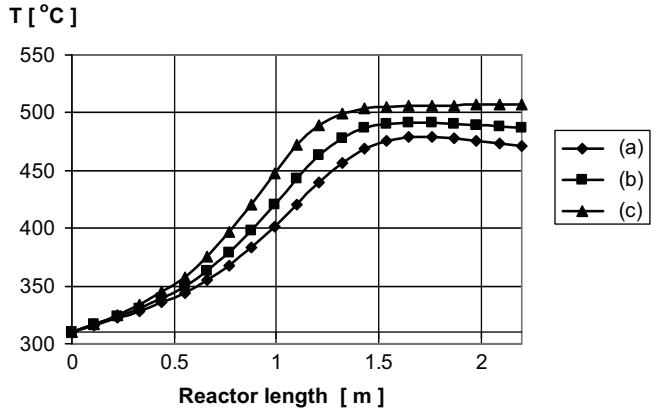

Fig. 3. Temperature profiles along the reaction zone (tube length $L = 2.2$ m) in the counter-current MR with the feasible membrane, filled with HTC, with steam to carbon ratio S/C = 3.25 (cf. items 2, 5 and 6 in Table 4), for various tube to shell and shell to surroundings heat transfer coefficients: (a) $h_{t-s} = h_{surr} = 0\ W\ m^{-2}\ K^{-1}$, (b) $h_{t-s} = h_{surr} = 5\ W\ m^{-2}\ K^{-1}$, and (c) $h_{t-s} = h_{surr} = 10\ W\ m^{-2}\ K^{-1}$.

3.3. Co- vs. counter-current MR

Temperature (T) and CO conversion (X) profiles for lower and higher S/C ratio, both for co- and counter-current MR are shown in Fig. 4. It can be seen that for the case discussed influence of configuration of flows in the tube and shell (i.e. co- vs. counter-current) at the end of the bed is negligible, while some differences of profiles may appear in the middle part.

An opinion about an advantage of counter- over co-current MR flows configuration can sometimes be found in the literature, however, e.g. in [27]. Simulations being carried out for both: very high [1] and feasible (the present study) permeation through the membrane revealed, that configuration of flows has negligible influence on the MR operation. Because of the clear contradiction between those opinions the matter was investigated more deeply. It should be stressed, however, that the results presented

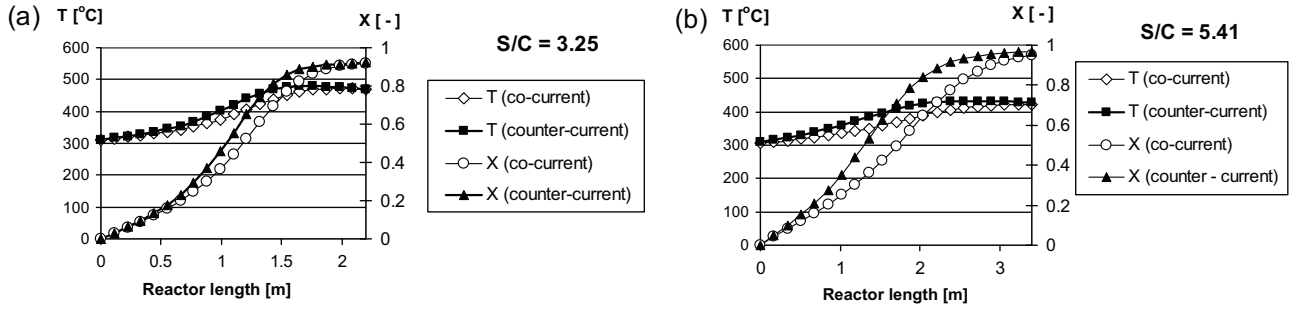

Fig. 4. Temperature and CO conversion profiles along the reaction zone (tube) in MR with the feasible membrane filled with HTC for co- and counter-current configuration of flows: (a) with lower steam flow rate (S/C = 3.25) and GHSV = 7813 h^{-1} (cf. items 2 and 7 in Table 4), (b) with higher steam flow rate (S/C = 5.41) and GHSV = 5477 h^{-1} (cf. items 3 and 8 in Table 4).

in [27] were obtained for MR with the relatively low pressure of 0.21 MPa (2.1 bar) in the reaction zone. Thus, for the feasible membrane option a comparison was made by simulating MR with all parameters the same except the flow configuration (compare items 3 and 8 with 4 and 9 in Table 4). Graphic illustration of this comparison is shown in Figs. 4 and 5. For high pressure of 2.6 MPa (26 bar) near the MR outlet it is difficult even to distinguish molar fraction and temperature profiles in the tube for co- and counter-current MR. When the shell side is taken into account, counter-current profiles for molar fractions (Fig. 5b) and temperature there (Fig. 5c) create mirror copies of nearly the same profiles appearing in the co-current configuration. However, for the pressure as low as 0.21 MPa there are visible differences in temperature and especially conversion profiles shown in Fig. 6. They really reveal a clear advantage of the counter-current option. This finding is obvious when one takes into account that influence of H_2 partial pressure in the shell P_{s,H_2} on the permeation driving force term: $[P^n_{t,H_2} - P^n_{s,H_2}]$ in Eq. (4) is higher, the lower is total pressure in the tube. Thus, when H_2 partial pressure in the tube P_{t,H_2} is high, due to high total pressure there, change of the partial pressure P_{s,H_2} caused by the reverse direction of flow in the shell becomes meaningless. When the pressure in the tube is low, MR should be much longer. Simulations were carried out for 12 m long MR, and in spite of that reaction mixture at the outlet appeared to be still rather far from equilibrium (see values of DFE_{out} at items 4 and 9 in Table 4). To some extent, perhaps, it could be caused by underestimation of the reaction rate, calculated using the kinetic parameters which were adequate to the industrial catalyst designed for the industrial WGS conversion, thus, obtained by experiments in high pressure. Even if the simulations performed for low pressure in the reaction zone are not very precise, they reveal, however, that significant difference between co- and counter-current configuration may appear only for relatively low pressure in the reaction zone of WGS MR.

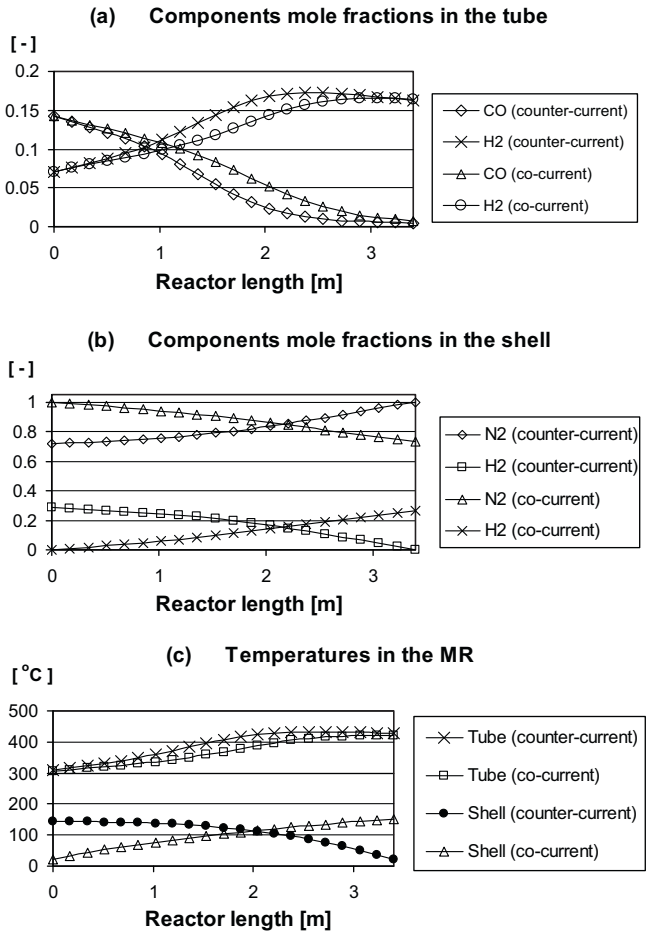

Fig. 5. Main gas component profiles (a) and (b) and temperatures (c) in the tube and shell side in MR with the feasible membrane filled with HTC with higher steam flow rate (S/C = 5.41) and GHSV = 5477 h^{-1} (cf. items 3 and 8 in Table 4) for co- and counter-current configuration of flows.

4. Simulations for some other solutions than single step MR

Having in mind obvious drawbacks of a single step MR (as shown in Fig. 1a) with a feasible membrane, it was decided to make a rough estimation whether some other options of MRs would not improve the hydrogen recovery in the unit. Thus pre-

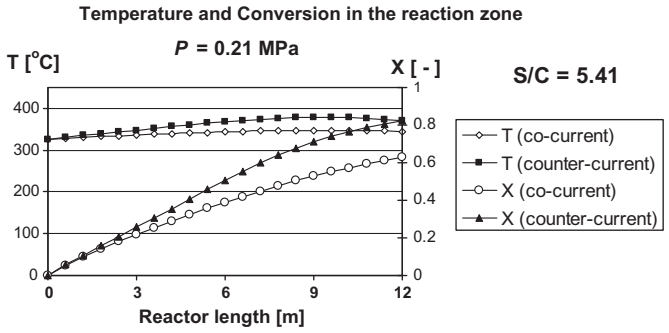

Fig. 6. Comparison of temperature and CO conversion profiles along the reaction zone (tube) in MR with the feasible membrane filled with HTC for co- and counter-current configuration of flows with the low pressure of 0.21 MPa (2.1 bar) in the reaction zone (cf. items 4 and 9 in Table 4).

Table 5
Chosen simulation results of the reactor schemes with two reaction zones shown in Fig. 7.

Option	L_1 [m]	L_2 [m]	L_3 [m]	S/C [–]	X [–]	DFE_{out} [–]	R_{H_2} [–]
(a) MR with conventional "pre-shift"	0.6	1.4	–	2.78	0.971	0.7427	0.216
(b) Two-step MR configuration	1.0	2.5	–	4.87	0.9403	0.8030	0.226
(c) Two-step MR configuration with separation zone between	1.5	3.0	1.5	5.41	0.9564	0.5717	0.532

Table 6
Comparison of results for HTC MR high and feasible membrane permeation.

High H_2 permeation (according to [1])					Feasible H_2 permeation (present study)				
S/C [–]	L [m]	X [–]	DFE_{out} [–]	R_{H_2} [–]	S/C [–]	L [m]	X [–]	DFE_{out} [–]	R_{H_2} [–]
1.01	1.0	0.6833	0.096	0.836	3.25	2.2	0.909	0.089	0.255
2.43	1.2	0.9477	0.632	0.963	5.41	3.4	0.963	0.156	0.344

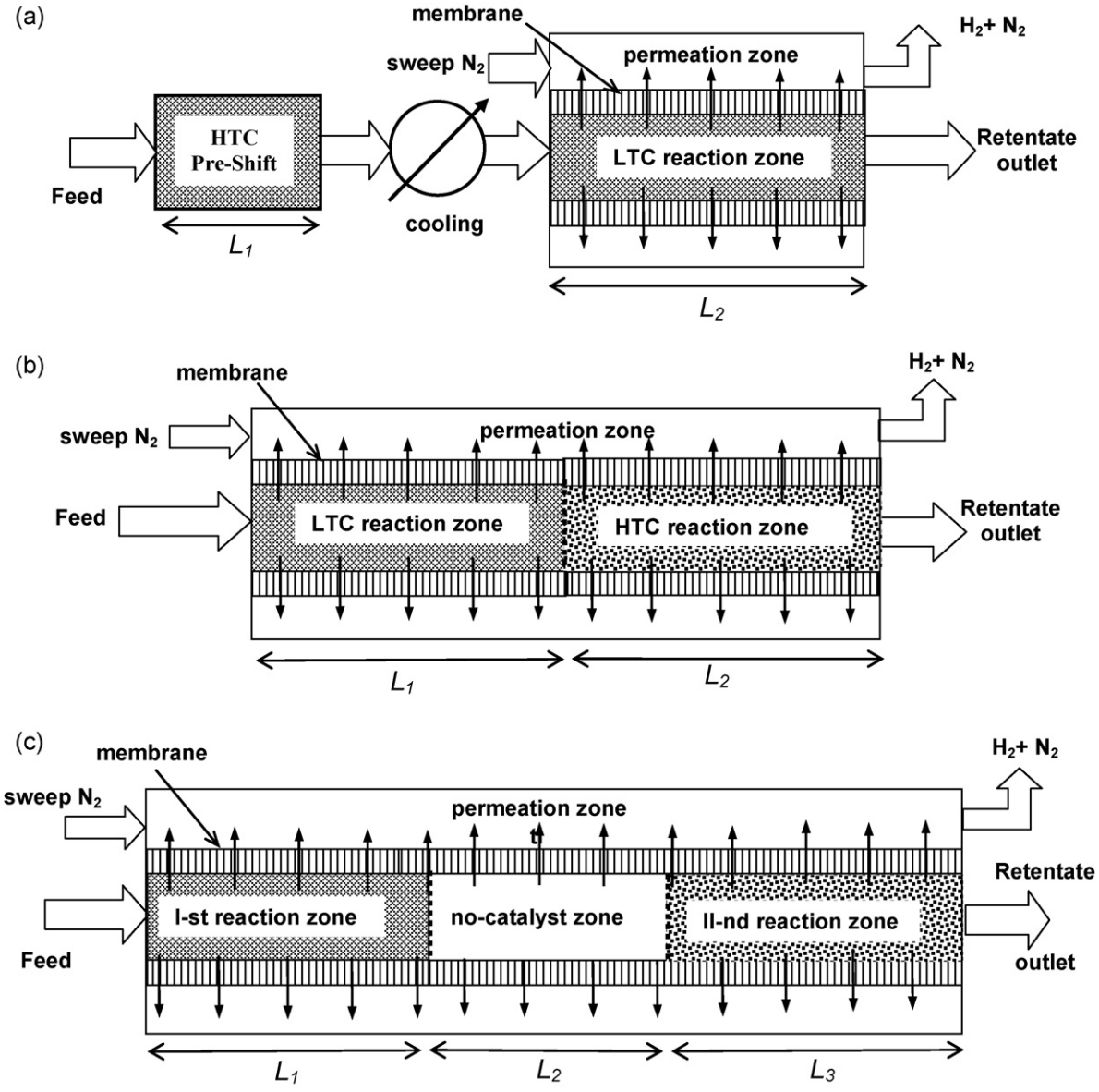

Fig. 7. Block diagrams of the two-step WGS configurations as an alternative to the single-step MR.

liminary simulations were made for the following two-step WGS configurations:

(a) first step with conventional high temperature "pre-shift" and after cooling MR as the second step (as proposed in [18]) – see Fig. 7a;
(b) two-step MR configuration with LTC in the first step and HTC in the second without heat exchange between them – see Fig. 7b;
(c) two-step MR configuration with no-catalyst membrane separation zone between them – see Fig. 7c.

Several variants were calculated for each option to get only a preliminary assessment of their practical applicability, but without any optimisation approach, however. The most representative results are shown in Table 5, where only these simulation variants revealing conversion ratio higher than 90% are presented.

These simulations revealed, that none of these solutions deliver the desired result due to lack of clear advantage over a single-step MR, especially when the hydrogen recovery R_{H_2} is taken into account. Therefore, these configurations were not deeply investigated.

5. Discussion

As it was clearly shown in [1] the composition of the coal-derived gas is significantly different from that derived from the other syngas technologies. Thus the results and discussion presented here refer only to WGS processing of the gas obtained from coal gasification, especially from technologies producing gas rich in CO. No study was made here for WGS MR processing syngas produced by other technologies, e.g. by steam reforming or partial oxidation, but one can easily presume that situation in such cases may be completely different and conclusions from the present study will be no longer valid. The goal of simulations presented was to estimate real effects, which can be achieved when MR is fed with coal-derived gas, and when a feasible membrane permeation is assumed in the simulation. A brief comparison of results for high (taken from [1]) and feasible permeation is shown in Table 6.

6. Conclusions

- Simulations for membrane with a very high permeation published in [1] were too optimistic. For moderate S/C = 2.43 high CO conversion and high hydrogen recovery (both well above 90%) could have been easily obtained. Simulation for feasible permeation parameters (taken from [23]) revealed, however, that in order to get high conversion above 90% a relatively high S/C should be applied. Moreover the hydrogen recovery is still low (below 30%) so for hydrogen production an additional H_2 separation unit (e.g. membrane or PSA) after the MR should have been applied. Thus, the results were less optimistic than it was in the former case of very high permeation presented in [1].
- When the feasible permeation parameters were applied it also appeared, that in order to get a high conversion the MR should be much longer.
- When a heat exchange between reaction and permeation zones is taken into account it occurs that this effect can have important influence on temperature profiles in the MR due to larger heat exchange area. It was difficult to estimate how high real heat transfer coefficients through the membrane can be expected. It is important, however, than for further development of the MR technology for the coal-derived gas, this phenomenon could be very useful. This cooling effect, if only high enough, could lessen reported in [1] demand for a very wide operating temperature range of the catalyst used in the MR.
- Comparison of co- vs. counter-current MR option has revealed that clear advantage of counter- over co-current configuration appears for low pressure in the reaction zone only. Since simulations performed in the present study assumed rather high pressure of 2.6 MPa (≈26 bar) in the tube and atmospheric in the shell, the difference of the outlet parameters between both flow configurations was insignificant.
- Results for other than single step MR configurations also presented in the paper allowed to presume that such solutions would not give, perhaps, any substantial improvement in the case of WGS coal-derived gas processing in MR.
- Concluding, it can be stated that future successful application of MRs for coal-derived gas depends on development of not only new catalysts (cf. [1]) with adequately wide operational temperature range, but also membranes with a high enough permeability and relatively high heat transfer coefficients.

Acknowledgement

This study was financed by the Polish Ministry of Science and Higher Education (Project PBZ-MEiN-2/2/2006).

References

[1] K. Gosiewski, K. Warmuzinski, M. Tanczyk, Catalysis Today 156 (2010) 229–236.
[2] A.S. Damle, S.K. Gangwal, V.K. Venkataraman, Gas Separation and Purification 8 (1994) 101–106.
[3] C. Hermann, P. Quicker, R. Dittmeyer, Journal of Membrane Science 136 (1997) 161–172.
[4] A. Basile, G. Chiappetta, S. Tosti, V. Violante, Separation and Purification Technology 25 (2001) 549–571.
[5] G. Barbieri, A. Brunetti, T. Granato, P. Bernardo, E. Drioli, Industrial and Engineering Chemistry Research 44 (2005) 7676–7683.
[6] A. Brunetti, A. Caravella, G. Barbieri, E. Drioli, Journal of Membrane Science 306 (2007) 329–340.
[7] M.E. Adrover, E. López, D.O. Borio, M.N. Pedernera, Chemical Engineering Journal (2009), doi:10.1016/j.cej.2009.04.057.
[8] M.E. Ayturk, N.K. Kazantzis, Y.H. Ma, Energy and Environmental Science 2 (2009) 430–438.
[9] S. Kumar, P.R. Shah, S. Shankar, S. Kumar, Journal of Chemical Reactor Engineering 4 (A5) (2006) 1–25.
[10] K.A. Hoff, J. Poplsteinova, H.A. Jakobsen, O. Falk-Pedersen, O. Juliussen, H.F. Svendsen, International Journal of Chemical Reactor Engineering 1 (A9) (2003) 1–12.
[11] N.C. Markatos, E. Vogiatzis, K. Koukou, N. Papayannakos, Trans IChemE, Part A, Chemical Engineering Research and Design 83 (A10) (2005) 1171–1178.
[12] J. Smit, G.J. Bekink, M. van Sint Annaland, J.A.M. Kuipers, Chemical Engineering Science 62 (2007) 1239–1250.
[13] J. Smit, G.J. Bekink, M. van Sint Annaland, J.A.M. Kuipers, Chemical Engineering Science 62 (2007) 1251–1262.
[14] J. Smit, M. van Sint Annaland, J.A.M. Kuipers, Chemical Engineering Science 60 (2005) 6971–6982.
[15] C.S. Patil, Membrane reactor technology for ultrapure hydrogen production (PhD Thesis), University of Twente, Enschede, The Netherlands (2005) p. 245.
[16] C.S. Patil, M. van Sint Annaland, J.A.M. Kuipers, Chemical Engineering Science 62 (2007) 2989–3007.
[17] A.S. Damle, T.P. Dorchak, Journal of Energy and Environmental Research 1 (2001) 77–89.
[18] M. Bracht, P.T. Alderliesten, R. Kloster, R. Pruschek, G. Haupt, E. Xue, J.R.H. Ross, M.K. Koukou, N. Papayannakos, Energy Conversion and Management 38 (1997) S159–S164.
[19] M.C. Carbo, D. Jansen, W.G. Haije, A.H.M. Verkooijen, Advanced membrane reactors for fuel decarbonisation in IGCC: H_2 or CO separation? in: 5th Annual Conference on Carbon Capture and Sequestration, Alexandria, VA, USA, 2006, pp. 1–15.
[20] gPROMS Introductory User Guide, Process Systems Enterprise Ltd., 2004, p. 254.
[21] Ideal physical properties foreign object (IPPFO), ippfo_documentation.pdf (Version 2.3.4) ed., Process Systems Enterprise Ltd.
[22] R.J. Kee, G. Dixon-Lewis, J. Warnatz, M.E. Coltrin, J.A. Miller, The Chemkin Thermodynamik Database, Sandia National Laboratories, Livermore, 1990.

[23] S.-K. Ryi, J.-S. Park, S.-H. Kim, S.-H. Cho, D.-W. Kim, K.-Y. Um, Separation and Purification Technology 50 (2006) 82–91.
[24] Polish catalysts producer's web page, Instytut Nawozów Sztucznych (Fertilizers Research Institute), http://www.ins.pulawy.pl/EN/index.php/content/view/113/114/.
[25] A. Gołębiowski, K. Stołecki, Chemik 3 (1998) 72–73.
[26] G. Madia, G. Barbieri, E. Drioli, Canadian Journal of Chemical Engineering 77 (1999) 698–706.
[27] W.W.S. Ho, Development of novel water–gas-shift membrane reactor, in: Hydrogen, Fuel Cells, and Infrastructure Technologies, DOE, 2003 (FY 2003 Progress Report), pp. 1–5.